Annals of Clinical Microbiology www.acm.or.kr

Original article

Laser scattering signal amplification and deep learning for detection of *Candida* culture positivity in women with vaginal symptoms: a preliminary analytical and pilot clinical evaluation

Jeong Su Park[1,*], Jehada-Inn Alihuddin[2,*], Kidong Kim[2,3], Kyoungman Cho[4], Jung-A Shin[1], Mulbora Jee[2]

[1]Department of Laboratory Medicine, Seoul National University Bundang Hospital, Seongnam, Korea
[2]Department of Obstetrics and Gynecology, Seoul National University Bundang Hospital, Seongnam, Korea
[3]Department of Obstetrics and Gynecology, Seoul National University College of Medicine, Seongnam, Korea
[4]The Wavetalk Co., Ltd., Daejeon, Korea

[*]These authors contributed equally as co-first authors.

Abstract

Background: Accurate diagnosis of vulvovaginal candidiasis (VVC) is challenging because of the limitations of conventional wet-mount microscopy, which requires a trained examiner and offers suboptimal sensitivity. This preliminary study evaluated the analytical performance of laser scattering signal amplification (LSSA) combined with deep learning and its preliminary clinical feasibility for detecting Candida culture positivity in women with vaginal symptoms.

Methods: LSSA signal data were acquired using the Bacometer from reference strains of five *Candida* species (10^2–10^5 colony-forming units (CFU)/mL in Luria–Bertani broth). A two-stage convolutional neural network (CNN) classifier was developed: Model 1 discriminated negative, *C. albicans*-positive, and non-albicans-positive specimens; Model 2 distinguished *C. albicans* from *C. tropicalis* among the positive specimens. The models were trained on 320 and 80 vials using 60:15:25 stratified splits and 5-fold cross-validation. Twenty vaginal discharge specimens from women with suspected VVC were assessed using fungal culture as the reference standard.

Results: Model 1 achieved a hold-out accuracy of 73.8% (95% confidence interval [CI] 62.7–83.0%) for three-class concentration discrimination, whereas Model 2 achieved 77.8% (95% CI 60.8–89.9%) in cascade evaluation. In the pilot clinical evaluation (5 culture-positive and 15 culture-negative specimens), the classifier correctly identified 1 of 5 culture-positive cases (sensitivity 20.0%, 95% CI 0.5–71.6%) and all 15 culture-negative specimens (specificity 100.0%, 95% CI 78.2–100.0%), yielding an overall accuracy of 80.0% (95% CI 56.3–94.3%), positive predictive value (PPV) 100.0% (95% CI 2.5–100.0%), and negative predictive value (NPV) 78.9% (95% CI 54.4–93.9%).

Conclusion: This preliminary study observed that concentration- and species-related scattering signals were partially classifiable under controlled reference strain conditions; however, the clinical sensitivity was insufficient (20.0%) in its current form. Correction of the sample pre-processing protocol is required before further clinical evaluation.

OPEN ACCESS

pISSN : 2288-0585
eISSN : 2288-6850

Ann Clin Microbiol 2026 June, 29(2):9
https://doi.org/10.5145/ACM.2026.29.2.9

Correspondence to
Kidong Kim
E-mail: kidong.kim.md@gmail.com

Received: April 13, 2026
Revised: May 29, 2026
Accepted: June 04, 2026

Keywords: *Candida*; Candidiasis, Vulvovaginal; Deep learning; Diagnosis; Laser scattering signal amplification

Introduction

Vulvovaginal candidiasis (VVC) affects millions of women worldwide and poses a significant public health burden [1]. The infection commonly causes vaginal itching, irritation, abnormal discharge, and dyspareunia, affecting 70–75% of women at least once in their lifetime [1–4]. Globally, recurrent VVC, defined as four or more episodes per year, affects approximately 138 million women annually and 372 million women over their lifetimes [5]. This widespread prevalence results in major health, economic, and quality-of-life challenges for the affected individuals [3,5].

Serious fungal infections, including VVC, are an important healthcare concern [6]. The prevalence of recurrent VVC has reached 3,810 cases per 100,000 women [7]. Long-term surveillance data from a university hospital between 2011 and 2022 revealed a steady increase in *Candida* positivity rates, with detection rates being the lowest in December and January, suggesting the potential influence of environmental factors [8].

Candida albicans remains the predominant etiologic agent of VVC, accounting for 80–90% of cases [9–12]. However, infections caused by non-albicans *Candida* (NAC) species, such as *Nakaseomyces glabratus* (formerly *C. glabrata*), *C. tropicalis*, *C. parapsilosis*, and *Pichia kudriavzevii* (formerly *C. krusei*), are increasing [3,13–16]. NAC species often exhibit reduced susceptibility to conventional antifungal agents, which complicates their clinical management [3,14]. Recent epidemiological data from Korea show that, since 2020, the detection frequency of NAC species has surpassed that of *C. albicans*, with *N. glabratus* emerging as the most prevalent species [8].

Accurate and rapid diagnosis of VVC is essential for its effective management; however, existing diagnostic methods have several limitations [1]. Conventional wet-mount microscopy relies on identifying yeast cells in the vaginal discharge and provides rapid results; however, it is operator-dependent and prone to subjective interpretation [1,9]. Its sensitivity typically ranges from 40% to 60%, whereas that of Gram staining is approximately 65% [3]. Furthermore, in busy gynecological outpatient settings, attending physicians are frequently unable to perform microscopy themselves owing to time constraints, and maintaining dedicated trained personnel on standby solely for wet-mount reading is operationally impractical in many clinical laboratories. Although fungal culture remains the gold standard with high sensitivity, its 24–48-hour turnaround time delays treatment initiation [10].

Molecular diagnostic tools, such as polymerase chain reaction (PCR) and nucleic acid amplification tests (NAATs), have been developed to overcome these issues [11,12]. NAATs offer improved sensitivity and specificity compared with conventional microscopy [11] but remain limited by their high cost and restricted species coverage. For example, endpoint PCR assays demonstrate high specificity but only moderate sensitivity (~65%) [10]. The combination of expenses, technical complexity, and incomplete species identification limits their clinical utility.

Owing to these diagnostic constraints, clinicians often resort to empirical treatments that may be ineffective against NAC species and contribute to antifungal resistance [2,11]. There is a pressing need for an alternative diagnostic approach that delivers objective, examiner-independent results without specialized microscopy personnel.

Laser scattering signal amplification (LSSA) has recently been introduced as an advanced optical technique that enhances detection sensitivity by exploiting multiple scattering phenomena through a patented scattering amplification chamber. This technology amplifies the intensity and informational richness of the scattered light signals from microscopic particles. A recent study demonstrated its utility for rapid, culture-independent bacterial detection directly from urine samples using a deep-learning classifier [17].

Based on this principle, we hypothesized that LSSA could provide a fast, objective, and examiner-independent platform for detecting Candida culture positivity in women with vaginal symptoms. This study was designed as a preliminary analytical evaluation and pilot clinical feasibility study by applying an established LSSA platform with a previously validated convolutional neural network (CNN) architecture [17] for new clinical applications.

Materials and methods

Study design

This study was designed as a preliminary analytical evaluation and a pilot clinical feasibility study with two sequential objectives. First, in the analytical phase, we assessed whether an LSSA-based CNN classifier retrained from scratch on a *Candida*-specific reference strain dataset using a previously validated platform [17] could discriminate *Candida* concentration levels and species under controlled laboratory conditions. Second, the pilot clinical phase evaluated whether the classifier trained on the reference strains could be generalized to vaginal discharge specimens from women with symptoms suggestive of VVC. This study did not constitute a clinical validation study; the clinical component was intended only for preliminary feasibility testing. The primary outcome was the patient-level sensitivity and specificity of the LSSA-CNN classifier for detecting Candida culture positivity using fungal culture as the reference standard, reported with 95% confidence intervals. The secondary outcomes were: (i) species-level discrimination accuracy in the reference strain evaluation, (ii) reference-strain hold-out classification accuracy for each model, and (iii) pre-filtration versus post-filtration colony count comparison.

Reference strains

Five reference strains of *Candida* were used: *Candida albicans* (ATCC 14053), *Nakaseomyces glabratus* (formerly *Candida glabrata*; KCTC 7219), *Candida tropicalis* (KCTC 7212), *Candida parapsilosis* (ATCC 22019), and *Pichia kudriavzevii* (formerly *Candida krusei*; ATCC 6258).

Culture conditions and inoculum preparation

Each strain was subcultured on Sabouraud Dextrose Agar (SDA) and incubated at 37 °C in a CO_2-free incubator for 24 h. A single colony was suspended in sterile normal saline and the turbidity adjusted to a 0.5 McFarland standard (approximately 2×10^6 CFU/mL). Suspensions were serially diluted tenfold to achieve final concentrations of 10^2, 10^3, 10^4, and 10^5 CFU/mL.

Experimental procedure with reference strains

Aliquots (25 µL) from each diluted suspension were added to 5 mL of Luria–Bertani (LB) broth to prepare working solutions with final concentrations of 10^2, 10^3, 10^4, and 10^5 CFU/mL. LB broth was selected because it provides a nutrient-rich, optically homogeneous background that supports microbial metabolic activity during the 30 min measurement period, thereby enhancing laser scattering signal generation while maintaining a stable optical baseline. Two milliliters of each working solution were transferred into measurement vials and placed into the instrument chamber preset at 30 °C. After 30 min of thermal stabilization, laser scattering image sequences were automatically acquired concurrently using a Bacometer (The Wavetalk Co., Ltd.); no additional acquisition time was required beyond the 30 min run (Fig. 1(B)). The device can simultaneously accommodate up to four vials.

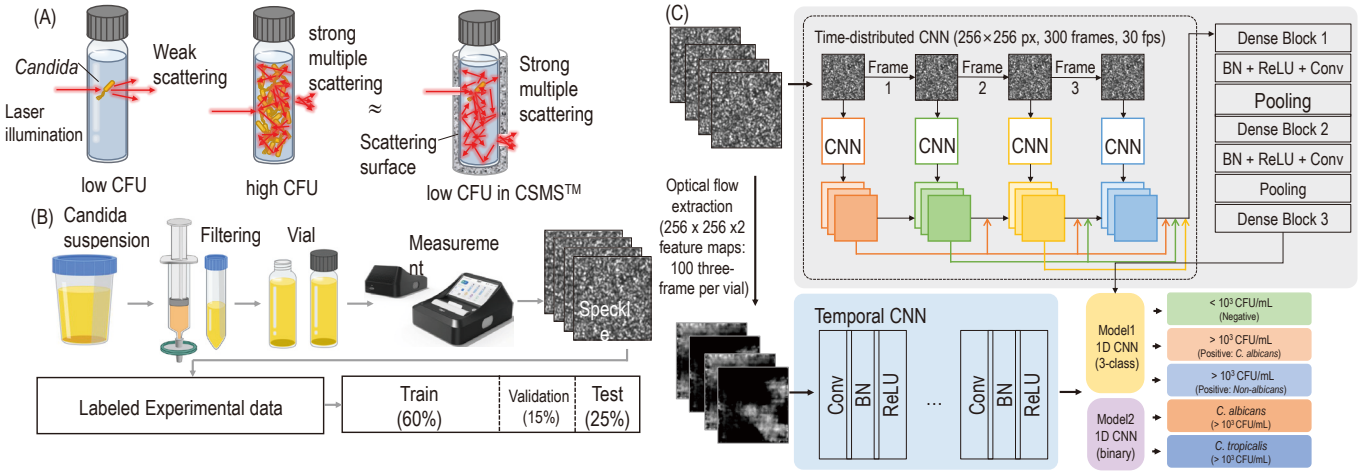

Fig. 1. Schematic of the laser scattering signal amplification (LSSA) platform and two-stream convolutional neural network (CNN) architecture for vulvovaginal candidiasis classification. (A) LSSA signal amplification principle. At low fungal cell concentration, incident light undergoes weak scattering through the sample vial. At high fungal cell concentration, the same light undergoes strong multiple scattering. The Bacometer's scattering chamber (CSMS™) provides an amplification surface so that even samples with low fungal cell counts produce strong multiple scattering equivalent to samples with high fungal cell counts without the chamber. (B) Clinical specimen measurement workflow. Vaginal discharge specimens are filtered through a 0.45-µm membrane filter; the filtrate is transferred to a glass vial, serially diluted (undiluted, 1:10, 1:100, 1:1000), and inserted into the Bacometer (The Wavetalk Co., Ltd.). The Bacometer captures 300 consecutive speckle images (256 × 256 pixels) over a 10-s window at 30 fps following 30 min thermal stabilization at 30°C. (C) Two-stage deep-learning classifier. Speckle image sequences are converted into 2-channel optical-flow feature maps (256×256×2; 100 three-frame chunks per vial) and processed by a two-stream CNN: a time-distributed spatial DenseNet (Dense Blocks 1–3, each followed by batch normalization [BN]+ReLU+Conv+Pooling) and a temporal DenseNet-based 1D CNN (Conv-BN-ReLU layers with global average pooling). Concatenated features are classified by Model 1 (3-class: Negative / Positive *C. albicans* / Positive Non-albicans) and, for Positive samples, by Model 2 (binary: *C. albicans* / *C. tropicalis*). Both models share the same network topology but were trained on entirely non-overlapping datasets (Model 1: 320 vials; Model 2: 80 vials). Layer-by-layer architecture specifications are provided in Supplementary Methods. CFU, colony-forming units.

Verification of viability in reference strains

Colony growth was subsequently confirmed, and the nominal working concentrations used in the study are summarized in Supplementary Table S1.

Dataset composition and data splitting

The Model 1 reference strain dataset comprised 320 vials (*C. albicans*, 160 vials; four non-albicans species, 40 vials each), generating 96,000 speckle frames in total. Model 2 comprised 80 vials (*C. albicans*, 40; *C. tropicalis*, 40) that generated 24,000 frames. Both datasets were partitioned using vial-level class-stratified splits as follows: training (60%), validation (15%), and holdout testing (25%). Within the 75% training-plus-validation pool, a stratified 5-fold cross-validation was applied at the vial level, ensuring that all 300 frames from a single vial were assigned exclusively to one fold. The hold-out test partition was isolated before model development and used exclusively for the final performance evaluation. The Model 1 and Model 2 datasets were acquired in independent experimental sessions without overlapping vials. The complete dataset compositions and split assignments are reported in Supplementary Table S1 (sub-tables S1a–S1d).

Model development using reference strains

A two-stage CNN classifier was developed to classify *Candida* species and concentration levels from 30 min laser scattering signal data, with the culture results serving as the reference standard. Speckle image sequences (300 frames per vial, 256 × 256 pixels, 30 fps over a 10-s acquisition window) were converted into 2-channel optical-flow feature maps (100 three-frame chunks per vial) and processed by a two-stream CNN: a time-distributed spatial DenseNet over raw speckle frames and a temporal DenseNet-based 1D CNN over optical-flow heatmaps with global average pooling. The features of both streams were concatenated before the final classification layer (Fig. 1(C)).

Model 1 performed three-class classification (Negative, $<10^3$ CFU/mL; Positive—*C. albicans*, $\geq 10^4$ CFU/mL; Positive—Non-albicans, $\geq 10^4$ CFU/mL). Samples classified as Positive by Model 1 were forwarded to Model 2, which is a binary classifier (*C. albicans* vs. *C. tropicalis*). Both models shared the same network topology but were trained on entirely non-overlapping datasets. All trainable weights were re-initialized and trained from scratch on the *Candida*-specific dataset; transfer learning from the prior urine-bacteria model weights [17] was not performed, as yeast cells generate substantially different scattering features compared to bacterial cells.

Hyperparameters were optimized by grid search over 25 combinations: learning rate $\in \{1\times10^{-3}, 5\times10^{-3}, 1\times10^{-4}, 5\times10^{-4}, 1\times10^{-5}\}$ × epochs $\in \{50, 100, 200, 500, 1000\}$; batch size fixed at 10. The Adam optimizer ($\beta_1 = 0.9$, $\beta_2 = 0.999$, $\varepsilon = 1\times10^{-7}$) was used. The final configuration selected by highest mean 5-fold validation accuracy was learning rate = 1×10^{-4} and epochs = 500 for both models. Model 1 used categorical focal loss ($\gamma = 2.0$; class-balanced $\alpha = [0.25, 0.50, 0.50]$ for Negative, Positive—C. albicans, and Positive—Non-albicans, respectively) to address the 2:1:1 class imbalance; Model 2 used standard binary cross-entropy. The complete grid search results are provided in the Supplementary Methods (Table SM1). The software frameworks were

Python 3.10, TensorFlow 2.12.0, and Keras 2.12.0. A random seed was set for weight initialization, data shuffling, and fold assignment, but was not formally archived in the training logs of the present study; this limitation is acknowledged in the Discussion section.

Clinical specimen acquisition

This study enrolled 20 women aged ≥19 years who presented consecutively to the gynecological outpatient clinic of Seoul National University Bundang Hospital (SNUBH) with clinical symptoms suggestive of VVC over a one-year enrollment period.

Inclusion criteria: (i) women aged ≥19 years; (ii) presenting with at least one symptom suggestive of VVC (vaginal discharge, itching, burning sensation, or other symptoms) as judged by the investigator; and (iii) provision of written informed consent.

Exclusion criteria: None. No formal exclusion criteria were applied, consistent with the exploratory specimen-collection design of this study.

After the insertion of a sterile speculum, the clinician visually examined the vaginal cavity and performed routine clinical evaluations. Five milliliters of sterile saline was instilled into the vagina, and the vaginal fluid was gently stirred with forceps to ensure thorough mixing. The pooled discharge was collected from the lower blade of the speculum using a needleless syringe. Two specimens were obtained from each patient: 2 mL for LSSA analysis and 1 mL for fungal culture.

Clinical specimens preparation

Each 2-mL vaginal discharge specimen was filtered through a 0.45-μm membrane prior to testing. The filtrate (i.e., the fraction that passed through the membrane) was used for LSSA, and the membrane-retained fraction was discarded. This filtration step was intended to remove debris and large particulates; however, as *Candida* yeast cells typically range from 3 to 8 μm in diameter—substantially larger than the 0.45-μm pore size—this procedure likely removed the majority of *Candida* organisms from the analyte, which is discussed as a critical limitation below.

Experimental procedure with clinical specimens

The filtered specimens were tested in parallel at four different concentrations (undiluted, 1:10, 1:100, and 1:1000). Two milliliters of each preparation were loaded into vials and analyzed under identical instrument conditions (30 °C, 30 min run). Because the Bacometer accommodates up to four vials simultaneously and each patient specimen requires four dilutions, one device processed one patient specimen per 30 min run. The total hands-on time per specimen, including sample collection, filtration, dilution preparation, and vial loading, was approximately 10 min, and the total turnaround time from specimen receipt to the result was approximately 40 min. A patient-level prediction was derived using an any-positive rule: a patient was classified as LSSA-Positive if any of the four per-vial predictions were positive; otherwise, the patient was classified as LSSA-Negative.

Decision rule for clinical specimens

Patient-level LSSA classification was determined using an any-positive rule applied across the four serial dilutions (undiluted, 1:10, 1:100, and 1:1000). A patient was classified as LSSA-positive if at least one per-vial prediction was positive; otherwise, it was classified as LSSA-negative. Species-level classification (*C. albicans* vs. non-albicans) was derived from Model 2 for LSSA-positive patients.

Microbiological verification of clinical specimens

To confirm microbial viability and evaluate the effect of filtration on organism recovery, aliquots of 10 μL and 100 μL were taken both before and after filtration from each specimen and plated on SDA. The plates were then incubated at 30 °C in a CO_2-free incubator for at least 24 h. Colony counts (CFU/mL) were recorded for each condition. The clinical reference standard for defining *Candida* positivity was based on pre-filtration culture results. All culture-positive isolates were identified to the species level by matrix-assisted laser desorption/ionization time-of-flight (MALDI-TOF) mass spectrometry (VITEK MS, bioMérieux).

Statistical analysis

All diagnostic performance metrics—sensitivity, specificity, positive predictive value (PPV), negative predictive value (NPV), and overall accuracy—were calculated at the vial level for reference strain experiments and at the patient level for clinical specimens using culture results as the reference standard. All point estimates were reported with 95% confidence intervals (CIs), calculated using the exact Clopper–Pearson binomial method. For reference-strain performance metrics, confidence intervals were computed using scipy.stats (SciPy v1.11.0). Categorical variables were summarized as frequencies and percentages. Continuous variables are summarized as medians with interquartile ranges (IQR). No inferential statistical comparisons were performed between groups. All analyses were conducted in Python 3.10 (Python), TensorFlow 2.12.0, Keras 2.12.0, and SciPy v1.11.0.

Results

Patient characteristics

The median age of the 20 enrolled women was 49.5 years (IQR 44–55 years; range, 29–63 years). Thirteen women (65.0%) were premenopausal, six (30.0%) were postmenopausal, and the menopausal status was unknown in one patient receiving gonadotropin-releasing hormone agonist therapy. The most common presenting symptom was vaginal discharge (15/20, 75.0%), followed by itching (10/20, 50.0%). Four women (20.0%) had diabetes mellitus. None of the patients had received antibiotics within the preceding two weeks; one patient (5.0%) had received antifungal therapy within the preceding 2 weeks. One patient (5.0%) had performed vaginal douching within the preceding 1 week. Patient characteristics, LSSA versus culture cross-tabulation, and diagnostic performance metrics are summarized in Table 1, and individual specimen results are provided in Supplementary Table S2.

Table 1. Summary of patient characteristics and pilot clinical evaluation results (n = 20)

Characteristic	Value
Age, years — median (IQR)	49.5 (44–55); range 29–63
Premenopausal	13 (65.0%)
Postmenopausal	6 (30.0%)
Unknown menopausal statusa)	1 (5.0%)
Diabetes mellitus	4 (20.0%)
Presenting symptoms	
Vaginal discharge	15 (75.0%)
Itching	10 (50.0%)
Other symptomsb)	4 (20.0%)
Recent medications	
Antifungal use within 2 weeks	1 (5.0%)
Antibiotic use within 2 weeks	0 (0.0%)
Vaginal douching within 1 week	1 (5.0%)
Candida culture vs. LSSA prediction	
Culture positive / LSSA positive (TP)	1
Culture positive / LSSA negative (FN)	4
Culture negative / LSSA positive (FP)	0
Culture negative / LSSA negative (TN)	15
Diagnostic performance (95% CI)	
Sensitivity	20.0% (0.5–71.6%)
Specificity	100.0% (78.2–100.0%)
PPV	100.0% (2.5–100.0%)
NPV	78.9% (54.4–93.9%)
Overall accuracy	80.0% (56.3–94.3%)

[a)]One patient receiving gonadotropin-releasing hormone agonist therapy.
[b)]Other symptoms: perineal redness, atrophic vaginitis, odor.
Individual specimen results are provided in Supplementary Table S2. 95% CIs were calculated using the exact Clopper–Pearson binomial method.
Abbreviations: TP, true positive; FN, false negative; FP, false positive; TN, true negative; CI, confidence interval; PPV, positive predictive value; NPV, negative predictive value; LSSA, laser scattering signal amplification.

Reference-strain hold-out evaluation

The Model 1 reference strain dataset comprised 320 vials (96,000 speckle frames in total), and the Model 2 dataset comprised 80 vials (24,000 frames). Dataset composition by species, concentration level, and class-stratified split assignment is shown in Supplementary Table S1.

In the hold-out test set evaluation, Model 1 achieved an overall three-class classification accuracy of 73.8% (95% CI 62.7–83.0%; n = 80 vials). The class-specific performance metrics with 95% CIs are listed in Table 2. After excluding negative cases, Model 2, evaluated in a cascade manner (n = 36 reference-strain vials classified as Positive by Model 1), achieved a species-level discrimination accuracy of 77.8% (95% CI 60.8–89.9%) between *C. albicans* and *C. tropicalis*. The confusion matrices for both models are shown in Fig. 2(A) and 2(B).

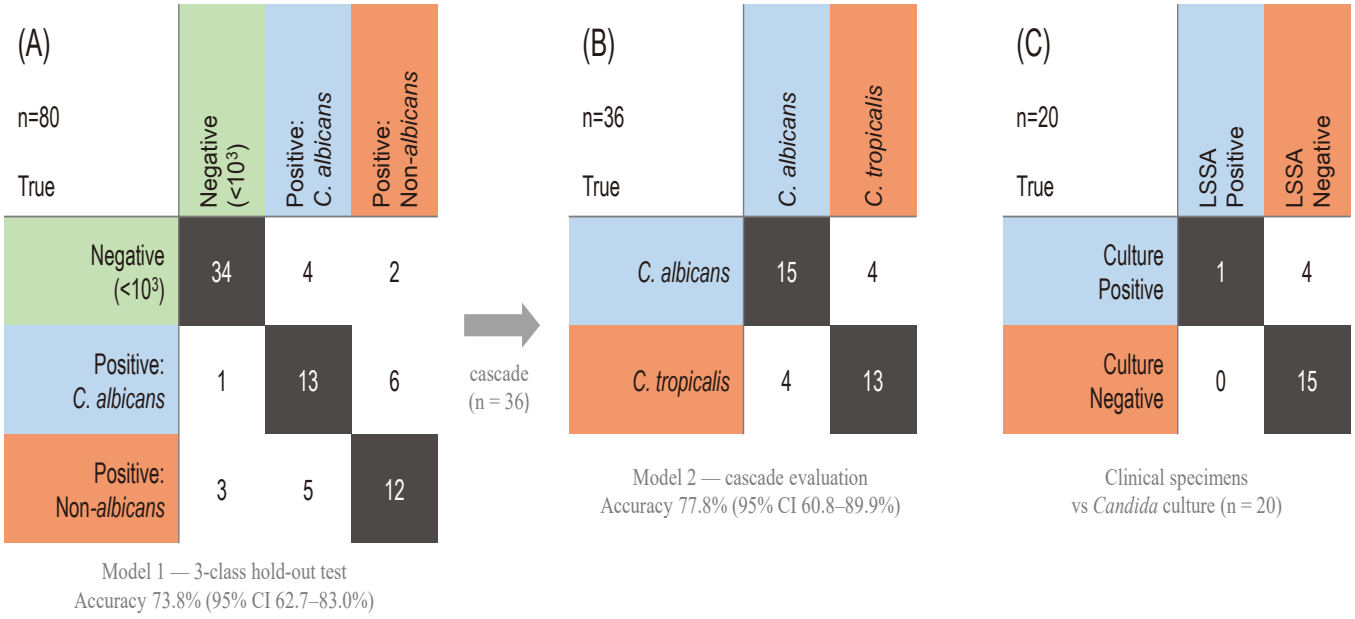

Fig. 2. Performance of the two-stage laser scattering signal amplification (LSSA) deep-learning classifier on hold-out reference-strain and preliminary clinical specimens. (A) Confusion matrix for Model 1, a three-class classifier (Negative, <10³ colony-forming units [CFU] /mL; Positive—*C. albicans*, ≥10⁴ CFU/mL; Positive—Non-albicans, ≥10⁴ CFU/mL), evaluated on the 25% hold-out test partition of the Model 1 reference-strain dataset (n = 80 vials; reference strains: *C. albicans* ATCC 14053, *N. glabratus* KCTC 7219, *C. tropicalis* KCTC 7212, *C. parapsilosis* ATCC 22019, *P. kudriavzevii* ATCC 6258). Rows indicate culture-confirmed true class; columns indicate model prediction. Overall accuracy: 73.8% (95% confidence interval [CI] 62.7–83.0%). (B) Confusion matrix for Model 2, a binary classifier (*C. albicans* vs. *C. tropicalis*), evaluated in a cascade manner on reference-strain samples predicted as Positive by Model 1 (n = 36; cascade evaluation). Overall accuracy: 77.8% (95% CI 60.8–89.9%). (C) Confusion matrix for the preliminary clinical evaluation, comparing patient-level LSSA prediction against the *Candida* culture result for 20 vaginal discharge specimens (5 *Candida* culture-positive, 15 *Candida* culture-negative). Absolute counts are printed inside each cell. Cell shading intensity is proportional to the cell count within each sub-panel. All 95% CIs were calculated by the exact Clopper–Pearson binomial method.

Table 2. Class-specific performance of the two-stage LSSA classifier on hold-out reference-strain test sets (exact Clopper–Pearson 95% CI)

Model	Class	Sensitivity (95% CI)	Specificity (95% CI)	PPV (95% CI)	NPV (95% CI)	F1 score
1[a)]	Negative (<10³ CFU/mL)	85.0% (70.2–94.3%)	90.0% (76.3–97.2%)	89.5% (75.2–97.1%)	85.7% (71.5–94.6%)	0.872
1[a)]	Positive: C. albicans (≥10⁴)	65.0% (40.8–84.6%)	85.0% (73.4–92.9%)	59.1% (36.4–79.3%)	87.9% (76.7–95.0%)	0.619
1[a)]	Positive: Non-albicans (≥10⁴)	60.0% (36.1–80.9%)	86.7% (75.4–94.1%)	60.0% (36.1–80.9%)	86.7% (75.4–94.1%)	0.600
1[a)]	Overall accuracy: 73.8% (95% CI 62.7–83.0%)					
2[b)]	*C. albicans*	78.9% (54.4–93.9%)	76.5% (50.1–93.2%)	78.9% (54.4–93.9%)	76.5% (50.1–93.2%)	0.789
2[b)]	*C. tropicalis*	76.5% (50.1–93.2%)	78.9% (54.4–93.9%)	76.5% (50.1–93.2%)	78.9% (54.4–93.9%)	0.765
2[b)]	Overall accuracy: 77.8% (95% CI 60.8–89.9%)					

[a)]Model 1: 3-class hold-out test (n = 80 vials). Non-*albicans* species: *Nakaseomyces glabratus* KCTC 7219, *C. tropicalis* KCTC 7212, *C. parapsilosis* ATCC 22019 and *Pichia kudriavzevii* ATCC 6258. Class-specific metrics using one-vs.-rest approach.

[b)]Model 2: binary cascade evaluation (n=36 vials predicted Positive by Model 1).

Abbreviations: LSSA, laser scattering signal amplification; CI, confidence interval; PPV, positive predictive value; NPV, negative predictive value; CFU, colony-forming units.

Pilot clinical evaluation

Of the 20 enrolled specimens, 5 were *Candida* culture-positive (all identified as *C. albicans* by MALDI-TOF mass spectrometry; pre-filtration colony counts: 10^3 to $>10^6$ CFU/mL) and 15 were *Candida* culture-negative. Routine bacterial culture was performed concurrently; bacteria were incidentally identified in some culture-negative specimens, but no systematic evaluation of bacterial vaginosis or *Trichomonas vaginalis* infection was performed.

Post-filtration counts were substantially reduced in all positive cases (range: 0 to 5×10^3 CFU/mL), confirming that 0.45-μm membrane filtration removed the majority of *Candida* organisms from the analyte. The single LSSA true-positive case (Case 4; post-filtration count: 5×10^3 CFU/mL) had the highest post-filtration count among all culture-positive specimens, consistent with a concentration-dependent detection threshold.

The LSSA classifier correctly identified 1 of 5 *Candida* culture-positive specimens (sensitivity 20.0%, 95% CI 0.5–71.6%) and all 15 *Candida* culture-negative specimens (specificity 100.0%, 95% CI 78.2–100.0%). The overall clinical accuracy was 80.0% (16/20; 95% CI 56.3–94.3%), positive predictive value was 100.0% (1/1; 95% CI 2.5–100.0%), and negative predictive value was 78.9% (15/19; 95% CI 54.4–93.9%). These results are summarized in Table 1; individual specimen-level results (culture results, species identification, pre- and post-filtration colony counts, and LSSA predictions for each of the 20 cases) are provided in Supplementary Table S2. The confusion matrix for the pilot clinical evaluation is shown in Fig. 2(C).

Discussion

This preliminary study evaluated the feasibility of an LSSA-based CNN classifier for detecting Candida culture positivity in women with suspected VVC. The results demonstrated moderate hold-out classification accuracy under controlled reference strain conditions but limited pilot clinical performance. Specifically, the LSSA-based CNN achieved hold-out test accuracies of 73.8% for three-class concentration-level discrimination (Model 1) and 77.8% for species-level discrimination between *C. albicans* and *C. tropicalis* in the cascade evaluation (Model 2), representing above-chance classification signals above the majority-class baseline (50.0%), but insufficient for clinical deployment. However, in the pilot clinical evaluation, the classifier detected only one of the five *Candida* culture-positive specimens despite correctly classifying all 15 *Candida* culture-negative specimens.

The high false-negative rate in clinical specimens is most likely attributable to the 0.45-μm membrane filtration applied during sample preprocessing. *Candida* yeast cells typically range from 3 to 8 μm in diameter—substantially larger than the 0.45-μm pore size—meaning the majority of organisms would have been retained on the membrane rather than passing into the filtrate used for LSSA analysis. This interpretation is strongly supported by the pre- and post-filtration colony count data: post-filtration counts were reduced to near-zero in 4 of 5 culture-positive cases, whereas the single true-positive case (Case 4) retained 5×10^3 CFU/mL post-filtration, the highest among all culture-positive specimens. This concentration-dependent pattern was consistent with the reference strain experiments, in which lower concentrations were associated with

higher misclassification rates. We identify the 0.45-μm filtration step as the primary methodological flaw in the current study, and its correction is the single most important prerequisite for any further clinical evaluation.

Although the total turnaround time of the LSSA system of approximately 40 min (10 min of hands-on preparation plus 30 min of automated acquisition) is longer than the 5–10 min required for wet-mount microscopy, the two methods differ fundamentally in their operational requirements. Wet-mount interpretation requires a trained and experienced examiner. In busy gynecological outpatient settings, attending physicians are frequently unable to perform microscopy themselves due to time constraints, while maintaining dedicated trained laboratory personnel on standby solely for wet-mount reading is operationally impractical. By contrast, LSSA image acquisition and CNN classification are fully automated and do not require trained examiners. The primary potential clinical advantage of LSSA, therefore, lies not in absolute turnaround time but in its capacity to deliver objective, examiner-independent results without requiring specialized microscopy personnel. However, the realization of this advantage requires the resolution of the sensitivity and sample preprocessing limitations identified in the present study.

A test with low sensitivity (20.0%, 95% CI 0.5–71.6%) and NPV (78.9%, 95% CI 54.4–93.9%) cannot serve as a rule-out test, as approximately 1 in 5 patients with a negative result would be a true positive—a clinically unacceptable miss rate. The corrected interpretation is that the observed specificity of 100.0% (95% CI 78.2–100.0%) and PPV of 100.0% (95% CI 2.5–100.0%); however, no false positives were observed in this small sample, and the PPV should be interpreted with caution given that it is based on a single true positive case and the 95% CI is very wide (2.5–100.0%).

The moderate reference strain accuracy (73.8% for Model 1) likely reflects both the inherent difficulty of discriminating optical scattering signals across *Candida* species and concentration levels and the limited dataset size. This level of accuracy is not indicative of severe overfitting because several design choices were made to mitigate this risk: categorical focal loss for class imbalance, stratified 5-fold cross-validation within the training pool, and pre-isolation of the hold-out test set before model development or hyperparameter selection. Rather, the 70% accuracy range reflects the early stage nature of this preliminary feasibility study and the inherent challenges of the task.

An additional factor contributing to the clinical-analytical performance gap is the morphological differences between the reference strains and *in vivo Candida* cells. The reference strains were cultured on SDA, yielding predominantly yeast cells (blastospores). In contrast, *C. albicans* frequently undergoes a morphological transition into hyphae and pseudohyphae in response to the host tissue environment, a process critical to its pathogenesis. Because laser scattering patterns are dependent on particle size, shape, and refractive characteristics, the scattering signatures of spherical yeast cells (3–5 μm) may differ fundamentally from those of elongated hyphal forms. This biological variance was not considered in the training model.

The LB broth used as the suspension medium for the reference strain experiments also did not closely replicate the physicochemical properties of clinical vaginal fluid. Differences in viscosity, refractive index, protein content, and background particle composition between the LB broth and vaginal discharge may introduce a systematic matrix discrepancy between the reference strain training data and clinical specimens. Future studies should evaluate alternative matrices, such as pooled negative vaginal wash fluids or validated

artificial vaginal fluid simulants, to produce clinically representative scattering signals.

Several important limitations must be acknowledged. First, the study included only 20 clinical specimens, of which 5 were *Candida* culture-positive, severely limiting the statistical precision of all performance estimates (wide 95% CIs). Second, the clinical reference standard was defined solely based on fungal cultures; no systematic evaluation of bacterial vaginosis, *Trichomonas vaginalis*, or other vaginitis etiologies was performed. The term "*Candida* culture-negative" therefore refers exclusively to the absence of *Candida* growth and does not imply clinical negativity. Third, formal calculations of area under the receiver operating characteristic curve and Cohen's kappa were not performed, given the small denominators and multiclass structure of Model 1; these metrics should be reported in future adequately powered studies. Fourth, the random seed for weight initialization and fold assignment was not formally archived, limiting exact reproducibility, which will be addressed in future work by archiving training codes and per-vial fold assignments in a public repository.

Before broader validation studies can be meaningfully designed, three specific re-optimization steps must be completed, and their impact on clinical sensitivity must be demonstrated experimentally. First, the sample preprocessing protocol must be corrected, and filtration should be replaced with an approach that preserves *Candida* cell integrity while removing interfering particulates, such as low-speed centrifugation with resuspension or larger-pore filtration, with reported pre- and post-processing culture counts to confirm organism recovery. Second, the matrix mismatch must be addressed by retraining the LSSA-CNN classifier using *Candida* suspensions prepared in pooled negative vaginal wash fluid or a validated artificial vaginal fluid simulant. Third, the morphological signal mismatch must be resolved by incorporating hyphae- and pseudohyphae-inducing culture conditions into model training to reflect the morphological diversity encountered in actual vaginal infections. Only after these three corrective steps have been implemented and shown to improve clinical sensitivity should large-scale prospective clinical evaluations with consecutive patient enrollment, standardized specimen collection, and culture-based reference standards be considered.

Ethics statement

This study was approved by the Institutional Review Board of Seoul National University Bundang Hospital (approval number: SNUBH IRB B-2306-836-301). Written informed consent was obtained from all participants.

Conflict of interest

The Bacometer device was provided free of charge by The Wavetalk Co., Ltd. Cho K, an employee of The Wavetalk Co., Ltd., participated in study design, model development, data analysis, and manuscript preparation. The Wavetalk Co., Ltd., through Cho K, therefore had involvement in these aspects of the study; however, the company had no role in patient sample collection, sample processing, clinical interpretation of results, or the decision to submit for publication. No other author has any employment, consulting, stock

ownership, patents, or other financial relationships related to the devices or technology. No other potential conflict of interest relevant to this article was reported.

Funding

This study was supported by a research grant from Seoul National University Bundang Hospital (grant number 02-2022-0031).

Acknowledgements

None.

Supplementary materials

The following supplementary materials are available on the journal's website:

- Supplementary Methods;
- Supplementary Table S1. Dataset composition and class-stratified split assignment for the two-stage LSSA deep-learning classifier;
- Supplementary Table S2. Individual clinical specimen results (n = 20).

Authors' contributions

Conceptualization: Park JS, Kim K, Cho K; Methodology: Park JS, Kim K, Cho K; Software: Cho K; Validation: Park JS, Kim K, Cho K, Shin JA; Formal analysis: Park JS, Alihuddin JI, Kim K, Cho K, Shin JA; Investigation: Park JS, Kim K, Cho K, Shin JA, Jee M; Resources: Park JS, Kim K, Cho K; Data curation: Shin JA, Jee M; Writing – original draft: Alihuddin JI, Kim K; Writing – review & editing: Park JS, Alihuddin JI, Kim K, Cho K, Shin JA, Jee M; Visualization: Cho K; Supervision: Kim K; Project administration: Kim K; Funding acquisition: Kim K

References

1. Wang Z, Wang R, Guo H, Zhao Q, Ren H, Niu J, et al. AI-assisted diagnosis of vulvovaginal candidiasis using cascaded neural networks. Microbiol Spectr 2025;13:e01691-24.
2. Martínez-García E, Martínez-Martínez JC, Martín-Salvador A, González-García A, Pérez-Morente MA, Álvarez-Serrano MA, et al. Epidemiological profile of patients with vulvovaginal candidiasis from a sexually transmitted infection clinic in southern Spain. Pathogens 2023;12:756.
3. Mondragón Rosas E, González Flores JE, Zamudio Carías AD, García Martínez N, Díaz Salcedo EX, Navarro López PE, et al. Pathogenesis and clinical management of vulvovaginal candidiasis in Mexican diabetic patients. Cureus 2025;17:e86012.

4. Ramazany Chaleshtori M, Madadian M, Akbari Sane A, Farzaneh F, Kazemi V, Montazer F, et al. Vaginal royal jelly for vulvovaginal candidiasis treatment: a randomized clinical trial. Adv Biomed Res 2025;14:32.
5. Denning DW, Kneale M, Sobel JD, Rautemaa-Richardson R. Global burden of recurrent vulvovaginal candidiasis: a systematic review. Lancet Infect Dis 2018;18:e339–47.
6. Seo HM, Kim SG, Kim JS. Real-world data of fungal infections in Korea: a comprehensive review of epidemiological studies. J Mycol Infect 2025;30:45–8.
7. Huh K, Ha YE, Denning DW, Peck KR. Serious fungal infections in Korea. Eur J Clin Microbiol Infect Dis 2017;36:957–63.
8. Hwang SY, Lim YK, Choe KW, Choi YH, Lee MK. Seasonality and epidemiological trends in species distribution and antifungal susceptibility of *Candida* species isolated from various clinical specimens conducted during 2011–2022, Korea: a retrospective surveillance study. Ann Clin Microbiol 2024;27:185–96.
9. Nguyen TBS, Nguyen HB, Le TXT, Bui THC, Nguyen LST, Nguyen TH, et al. Applying machine learning with MobileNetV2 model for rapid screening of vaginal discharge samples in vaginitis diagnosis. Sci Rep 2025;15:19171.
10. García-Salazar E, Betancourt-Cisneros P, Ramírez-Magaña X, Díaz-Huerta H, Martínez-Herrera E, Frías-De-León MG. Utility of Cand PCR in the diagnosis of vulvovaginal candidiasis in pregnant women. J Fungi 2025;11:5.
11. Chen J, Tse J, Shi L, Cheng MM, Lillis R, Near AM. Real-world clinical burden of patients presenting with vaginitis symptoms in the United States. AJOG Glob Rep 2025;5:100504.
12. Cornely OA, Sprute R, Bassetti M, Chen SCA, Groll AH, Kurzai O, et al. Global guideline for the diagnosis and management of candidiasis: an initiative of the ECMM in cooperation with ISHAM and ASM. Lancet Infect Dis 2025;25:e280–93.
13. Rodriguez E, Savid-Frontera C, Angiolini SC, Hernáez-Sánchez ML, Miró MS, Viano ME, et al. Type-I interferons in vulvovaginal candidiasis: mechanism of epithelial early defense and immune regulation against *Candida albicans*. Mucosal Immunol 2025;18:1124–38.
14. Nahuelcura F and Duarte EÁ. Species distribution, characterization, and antifungal susceptibility patterns of *Candida* isolates causing oral and vulvovaginal candidiasis in Chile. Antibiotics 2025;14:712.
15. Faraji R, Maleki A, Gheisoori A, Rashidi T, Salimi Mansouri A, Rashidi F, et al. Evaluation of epidemiological, clinical, and microbiological features of vulvovaginal candidiasis. GMS Hyg Infect Control 2025;20:Doc15.
16. Kroustali V, Kanioura L, Resoulai E, Siopi M, Antonopoulou S, Meletiadis J. Antifungal susceptibility testing and determination of local epidemiological cut-off values for *Candida* species isolated from women with vulvovaginal candidiasis. Microbiol Spectr 2025;13:e02488-24.
17. Lee KS, Lim HJ, Kim K, Park YG, Yoo JW, Yong D. Rapid bacterial detection in urine using laser scattering and deep learning analysis. Microbiol Spectr 2022;10:e01769-21.